

# Data Processing Methods for Mobile Indoor Navigation

Alexey Roienko  
*IT-Jim*  
Kharkiv, Ukraine  
a.roienko@it-jim.com

Feliks Sirenko  
*IT-Jim*  
Kharkiv, Ukraine  
sirenkofelix@gmail.com

Yevhen Chervoniak  
*IT-Jim*  
Kharkiv, Ukraine  
eugenecher94@gmail.com

Ievgen Gorovyi  
*IT-Jim*  
Kharkiv, Ukraine  
ceo@it-jim.com

**Abstract**—The competition on the world market of smartphones and tablets between the acknowledged leaders on one side and the numerous newcomers on the other makes them all look for new solutions that open additional opportunities for the developers and customers without the growth of the price. The progress with new opportunities turns possible when it happens simultaneously in the software and the hardware. The brightest one example of the above statement can be observed for the sensors of mobile devices. It is totally impossible to imagine modern smart devices having no sensors, as the progress of last decade (SLAM, face ID, OCR, pattern recognition etc.) was achieved thanks to considerable improvements of sensors and the algorithms for their processing. The paper addresses the questions of characteristics analysis of such mobile sensors as accelerometer, magnetometer and gyroscope from the point of view of their application in indoor navigation field. Signals of BLE beacons and their processing methods are investigated as well. The sensor fusion task is briefly discussed and several practical examples are given.

**Keywords**—*signal processing, sensor fusion, indoor navigation, BLE navigation, IMU navigation*

## I. INTRODUCTION

Mobile sensors have been coming into our life more and more. Besides, being used widely in smartphones, they started a new branch in mobile industry – wearable fitness-trackers and smart watches. Almost all leading technology companies, like Apple, Samsung or Xiaomi produce such devices and integrate them into their infrastructure. Moreover, mobile sensors are the basis for such modern and greatly developing fields like Augmented Reality (AR) where they serve, for example, for improving the detection of markers on the scene, or Virtual Reality - for precise head pose tracking. Another popular and important scientific area of mobile sensors application is known as Simultaneous Localization and Mapping or SLAM. Finally, indoor navigation, which can be considered as GPS for indoor environments, relies greatly on smartphone inertial sensors [1] - [8]. Despite the fact that there are many different sensor types, some of them are more common and greatly applied in the mentioned applications. Namely, they are accelerometer (A) which measures the linear acceleration of a device, magnetometer (M) that detects the Earth magnetic field along three axis of device coordinate system, and gyroscope

(G) which measure angular velocity. The combination of these three sensors, known as Inertial Measurement Unit (IMU), is widely used for determination of device pose in global coordinate system. It is worth noting that mobile sensors can be made of different quality. Recently, the so-called Micro-Electro-Mechanical Systems (MEMS) sensors have been attracted great interest. They are widely applied in smartphones and different wearable devices. As it will be shown, they can provide rather noisy signals but their main benefit is their accessibility due to the low price.

Besides the IMU, Wi-Fi access points and Bluetooth Low Energy (BLE) beacons can also be considered as sensors. Numerous companies, like Estimote, Infsoft, Senion and many others, offer their Software Development Kits, which utilize the signals from BLE and/or Wi-Fi sensors as well as IMU data for finding a user position as a solution of Indoor Navigation task. BLE and Wi-Fi data signals differ greatly from the inertial sensor data. While the IMU signals possessing long-term drift (G) or variations (M and A) because of different metal things or internal sensor noise but are rather accurate for short period of time [13] - [14], BLE signals in opposite allow obtaining small positioning error in long-term perspective, but fluctuate greatly around its true values. As a result, modern indoor navigation systems provide fusion of BLE and IMU data for their mutual improvement. Such solutions are known as Hybrid Indoor Localization and Navigation (HILN) systems [17]. The HILN system is a drift-free, low-cost, light-weight, easy-to-integrate IPS, enabling ubiquitous navigation of pedestrians in buildings equipped with beacons or Wi-Fi. The article is organized as follows. At first, features of A, M and G sensor signals are analyzed as well as signal processing methods for IMU-based navigation system are discussed in Section 2. Next, BLE sensor signals are investigated and methods for their processing are discussed. Section 4 is devoted to the fusion technique based on a particle filter. Finally, practical results of three mentioned positioning approaches are provided for comparative analysis.

## II. SIGNAL PROCESSING FOR THE IMU NAVIGATION

IMU as a combination of mainly three sensors, A, M and G, is a basis for inertial navigation system (INS) which is one of the important parts of Indoor Navigation systems. Usually INS determine a user position by implementing a Pedestrian Dead-Reckoning (PDR) algorithm [1] or its

numerous modifications (see for example [2]). At the first stage of the algorithm, a user step must be detected [3]. Next, the user step length is evaluated [6]-[8] followed by the attitude and heading estimation by one of the fusion algorithms. Finally, IMU readings are transformed from the local coordinate system to a global one using the determined device orientation angles [12]-[13]. Then the detected steps are summed up to get the user track in the building.

However, there are some challenges while designing INS. First of all the IMU readings are spoiled with noise. Let us show this fact by analyzing A and M sensor signals for the three test cases: #1. Smartphone lays on the table immovable; #2. User holds the device in hand and stays in static position; #3. User walks straight ahead. For comparative analysis, signals were harvested with Samsung Galaxy Note 5 (premium class smartphone) and Huawei P8 Lite 2017 (business class smartphone) and the mean square error (MSE) was calculated as an indicator of signal variations. It is worth noting that each sensor provides measurements as a 3D vector containing X, Y and Z axis component values of a parameter.

Results for A sensor data represented in Table I show that even in stationary cases there are fluctuations and their level depends on the smartphone class, i.e. the more expensive the smartphone, the better sensors are built in. The same results are obtained for M sensor data (see Table II). The difference between MSE values between test cases 1 and 2 is up to 5 times for Samsung Galaxy Note 5 and up to 7 times for Huawei P8 Lite 2017. It is worth noting that M readings suffer from numerous magnetic disturbances, which are available everywhere in modern buildings with their Wi-Fi spots and numerous obstacles made of steel.

TABLE I. ACCELEROMETER DATA MSE VALUES

| grav. units           | $a_x$  | $a_y$  | $a_z$  |
|-----------------------|--------|--------|--------|
| Test case 1           |        |        |        |
| Samsung Galaxy Note 5 | 0.0007 | 0.0007 | 0.0012 |
| Huawei P8 Lite 2017   | 0.0139 | 0.0157 | 0.0067 |
| Test case 2           |        |        |        |
| Samsung Galaxy Note 5 | 0.0176 | 0.0151 | 0.0199 |
| Huawei P8 Lite 2017   | 0.0374 | 0.0619 | 0.0403 |

From practical point of view, the most important results are observed for the test case #3 when user moves. Accelerometer vector absolute values represented in Fig. 1 show that the A sensor components are corrupted by noise. In order to find ways how to cope with that, the A signal spectrum was investigated (Fig. 2). It is seen that there is a harmonic at about 2 Hz which corresponds to the signal oscillations due to the user steps. At the same time, there are additional harmonics at the region from 5 to 10 Hz caused by the influence of sensor noise. Note that the amplitude levels as well as the number of spurious spectral components depend on the phone model.

The other important facts can be found from the analysis of the influence of user movement on characteristics of M data. Results provided in Table II show that the MSE values of M signal components are reasonably increased for both analyzed devices. The difference is up to 3 times comparing to the stationary case #2. It is obvious that effective noise filtering is the first challenge to overcome on a way to an accurate user positioning and tracking. Especially it is important for A data because of its application for user step

detection. The task of A sensor signal denoising has numerous solutions. They are the application of the Butterworth, Bessel, Chebyshev, Savitzky-Golay, moving average, Total Variation [18] or Kalman [19] filter.

TABLE II. MAGNETOMETER DATA MSE VALUES

| $\mu T$               | $m_x$  | $m_y$  | $m_z$  |
|-----------------------|--------|--------|--------|
| Test case 1           |        |        |        |
| Samsung Galaxy Note 5 | 0.0127 | 0.0109 | 0.0315 |
| Huawei P8 Lite 2017   | 0.0512 | 0.0418 | 0.0575 |
| Test case 2           |        |        |        |
| Samsung Galaxy Note 5 | 0.0574 | 0.0637 | 0.0263 |
| Huawei P8 Lite 2017   | 0.1696 | 0.2904 | 0.1021 |
| Test case 3           |        |        |        |
| Samsung Galaxy Note 5 | 0.3913 | 0.2370 | 0.2641 |
| Huawei P8 Lite 2017   | 0.5403 | 0.4350 | 0.3081 |

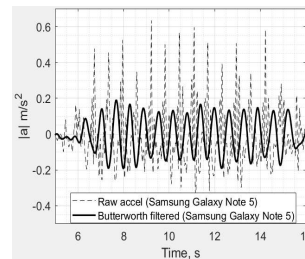


Fig. 1. The raw and filtered accelerometer signals for test case #3

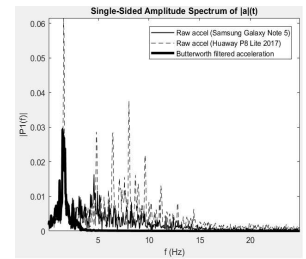


Fig. 2. Fourier spectrum estimates of the raw and filtered accelerometer signals for test case #3

The solutions differ from each other by the complexity, delay and quality of filtration. To our best knowledge there are no exact recommendations what algorithm must be used for the smartphone IMUs. Based on the held experiments, the highest performance for the A sensor was obtained from the Butterworth filter, which has the 'smoothest' frequency response in terms of having the most derivatives of its magnitude response being zero at the geometric center of the passband and the simplest transfer function in that the coefficients of the polynomial are easy to calculate. The result of filter application is shown in Figure 1 in temporal domain as well as in Figure 3 in spectral domain. It is clearly seen that the A signal becomes smoother due to the noise removal in high-frequency domain. It is known that MEMS gyroscope uses the Coriolis acceleration effect on a vibrating mass to detect angular rotation. The gyroscope measures the angular velocity, which is linear to rate of rotation. It responds quickly and accurately and the rotation can be computed by time-integrating the gyroscope output. But G sensor readings suffer from inertia. Without special treatment, the inertia causes the drift of the trajectory estimated by INS during the long tracks [13].

TABLE III. MSE OF GYROSCOPE VECTOR VALUES VARIATIONS

| Rad. / sec.           | $g_x$  | $g_y$  | $g_z$  |
|-----------------------|--------|--------|--------|
| Test case 1           |        |        |        |
| Samsung Galaxy Note 5 | 0.0001 | 0.0002 | 0.0001 |
| Huawei P8 Lite 2017   | 0.0015 | 0.0025 | 0.0210 |
| Test case 2           |        |        |        |
| Samsung Galaxy Note 5 | 0.0032 | 0.0027 | 0.0018 |
| Huawei P8 Lite 2017   | 0.0078 | 0.0095 | 0.0103 |
| Test case 3           |        |        |        |
| Samsung Galaxy Note 5 | 0.0204 | 0.0143 | 0.0131 |
| Huawei P8 Lite 2017   | 0.0211 | 0.0277 | 0.0441 |

MSE values for G sensor signal components for three test cases represented in Table III show that there are G signal deviations which are caused by internal sensor noise (Case 1), user hand trembling (Case 2) and user movement (Case 3). As an example of inertia influence Fig. 3 shows the dependence of rotation angle around X axis on time. The data recorded by the smartphone laid on the table and rotated on 90 degrees anticlockwise at first and then backward to initial position. It is clearly seen that there is an integration error about -3...-5 degrees when device was returned to initial position. The same effects are observed for other components in case of corresponding rotations. Neither A and M sensors nor G can be considered error-free. While A signal is usually used for user step detection, G and M as well as A are mainly applied for determination of device orientation angles. Such fusion algorithms like Madgwick, Mahoney and Kalman fusion filters [14] allow neglect the drawbacks of each sensor and use their data for improving the estimate of orientation angles.

### III. SIGNAL PROCESSING FOR THE BLE NAVIGATION

Another group of data processing methods deals with the signals from BLE beacons or Wi-Fi access points. They are known as Received Signal Strength Indicator (RSSI) signals. Practically, RSSI is a power of a received signal shifted by some offset value. Such signals do not suffer from the inertia, but are considerably influenced by fluctuations.

Note that the trilateration is a key method for user position estimation in beacons-based indoor navigation systems (**Error! Reference source not found.**). It requires at least three distances to the beacons near the user for its operation. Distances are obtained from the RSSI values received by application of the so-called, path-loss model [16], which represents the dependence of RSSI values on the distance between the smartphone and the corresponding beacon. Let's start the RSSI signal analysis with the investigation of number of received BLE packages. Test logs are recorded using Samsung Galaxy Note 5 device for the static test case when user stays immovable at the depicted (by diamond) point of the test room (Figure 5). There are nine installed BLE beacons, produced by Sensoro Comp.

The analysis of the so-called RSSI received package map (Figure 6a) shows that not all packages are received for each beacon (the missing packages are outlined with red rectangles). Moreover, the gaps in the RSSI signals result in misselection of the beacons.

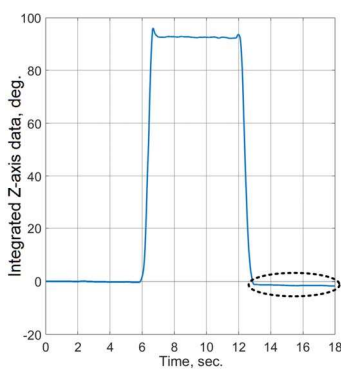


Fig. 3. The rotation angle around X device axis obtained by integrating G data values

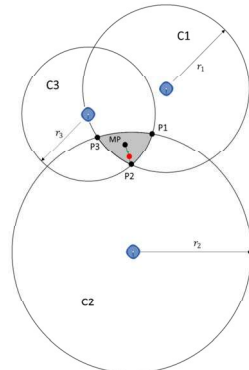


Fig. 4. Trilateration problem

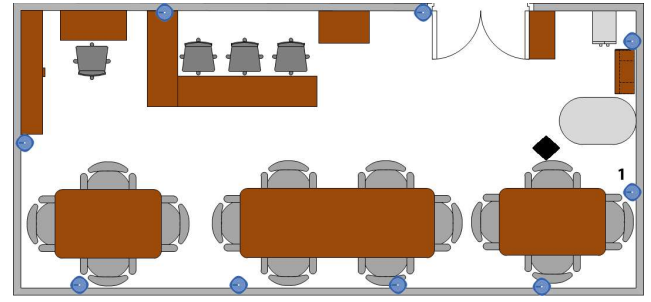


Fig. 5. Trilateration problem

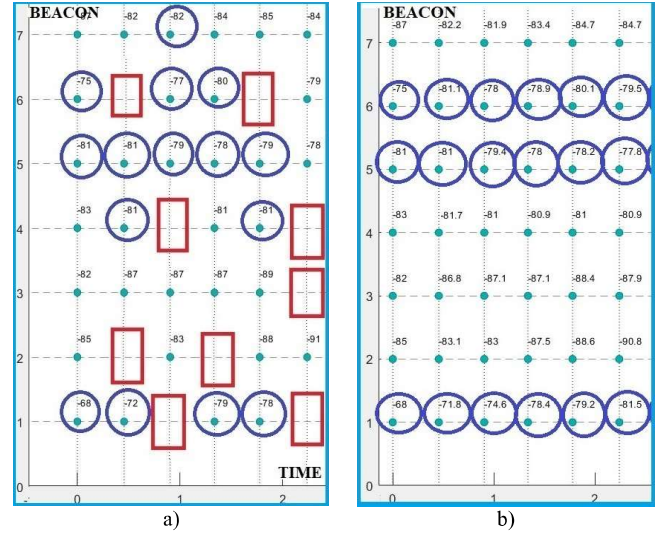


Fig. 6. RSSI package map before (a) and after Kalman filtering (b):  - missing packets,  - beacons with RSSI that are selected for trilateration

For example, the selected beacons at the first step are the beacons with numbers 1 5 and 6, at the second – 1,5 and 4, and at the third – 5, 6 and 7, which makes no sense at all because the user is not moving and it is reasonable to expect the same selected beacons at each time moment. As a result, there is a discontinuous user positioning and trilateration can be not possible for some time samples.

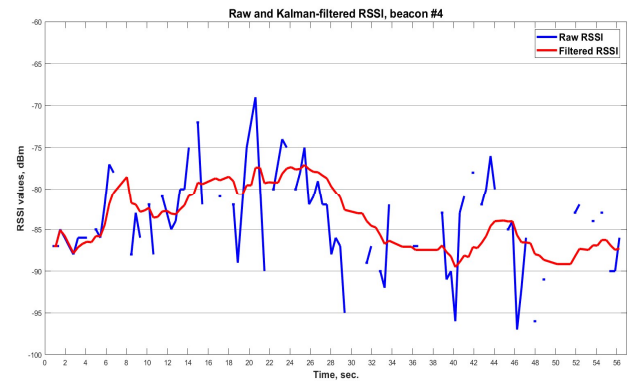


Fig. 7. Raw and Kalman-filtered RSSI signals for the beacon #4 in the test room

Next cornerstone of BLE signals is the great fluctuations of RSSI values on time for the given beacon. Figure 7 highlights this fact by an example of such a signal received from one of the beacons of the test room (Figure 5). As a result, the exact position can not be determined, and a user can be localized in some area only.

Both described challenges can be overcome by the Kalman filter for RSSI, described in [22]. The model of the process used in this case is

$$\begin{bmatrix} \text{RSSI}_i \\ \Delta \text{RSSI}_i \end{bmatrix} = \begin{bmatrix} 1 & \delta t_i \\ 0 & 1 \end{bmatrix} \begin{bmatrix} \text{RSSI}_{i-1} \\ \Delta \text{RSSI}_{i-1} \end{bmatrix} + \begin{bmatrix} v_i^{\text{RSSI}} \\ v_i^{\Delta \text{RSSI}} \end{bmatrix} \quad (1)$$

where  $\text{RSSI}_i$  and  $\text{VRSSI}_i$  are predicted values of RSSI and the RSSI's change rate for the  $i$ -th beacon;  $\delta t_i$  denotes time interval between current and previous received packages from the beacon;  $v_i^{\text{RSSI}}$  and  $v_i^{\text{VRSSI}}$  are random variables; and model of the measurement is

$$\text{RSSI}_i = \begin{bmatrix} 1 & 0 \end{bmatrix} \begin{bmatrix} \text{RSSI}_{\text{meas } i} \\ \Delta \text{RSSI}_{\text{meas } i} \end{bmatrix} + v_{\text{meas}}^{\text{RSSI}} \quad (2)$$

where  $\text{RSSI}_{\text{meas } i}$  and  $\text{VRSSI}_{\text{meas } i}$  are measured values of RSSI and the RSSI's change rate for the  $i$ -th beacon;  $v_{\text{meas}}^{\text{RSSI}}$  is a random variable.

D. Gusenbauer [22] showed that this method (1)-(2) was able to smooth the RSSI readings from all beacons. However, we found out that this filter could also serve as a useful tool to restore the missing packets with high confidence. For doing this, the following algorithm's modification is applied – Figure 8. As you can see in Figure 6b, there are no missing packets after filtration, which is the first but not the major achievement. The beacons for the trilateration will be selected correctly, i.e. we expect to observe no weird beacon “swaps”. The last thing achieved by the Kalman filtration is the smooth signal with no intense fluctuations (Figure 7).

#### IV. SIGNAL PROCESSING FOR HIL NAVIGATION

No doubts, that the IMU component of a HILN system is very accurate for up to 1 minute navigation. However, this is not typical for the navigation to last only few minutes.

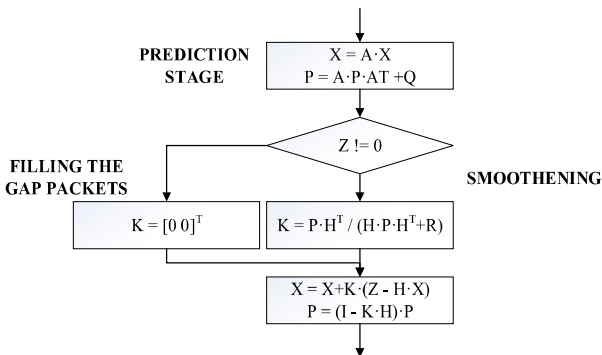


Fig. 8. The flow of Kalman filter for RSSI with restoring option:

$X = \begin{bmatrix} \text{RSSI}_i \\ \Delta \text{RSSI}_i \end{bmatrix}$  is a state matrix,  $A = \begin{bmatrix} 1 & \delta t_i \\ 0 & 1 \end{bmatrix}$  is a state-transition model,  $P$  is the covariance of the process noise,  $Z = \text{RSSI}_i$  is observation,  $H = \begin{bmatrix} 1 & 0 \end{bmatrix}$  is the observation model,  $Q$  and  $R$  are the covariance of the process and observation noise respectively.

Hence, it sounds reasonable to expect the INS to have corrections from time to time to eliminate the accumulated drift. The data for the correction is typically obtained from the non-inertial systems, like, for example, BLE or Wi-Fi.

There are several known methods for fusing the inertial and non-inertial navigation systems. Kalman filtering is a very powerful fusion tool able to automatically determine the trust rates to different sources. However, the monolite structure of the filter makes its modification to be a very complex task. For example, if a user walks near the wall with the accumulated drift to the wall side, then sooner or later user will find himself in the wall. The considered case is typical for long (>25 meters) and narrow (<3 meters) corridors. As the accuracy of BLE is less than 3 meters, then the correction will have never be effective. Hence, the most prospecting method for the fusion is a particle filter. The filter was first proposed in 1996 in [20] and since that time takes a considerable portion of cases that relate to Markov processes. The filtering has three stages that happen every iteration and one stage that happens once (in the ideal case) or several times.

Figure 9 represents a comparison of three different approaches used for indoor navigation system design as well as the ground-truth marked with arrows. In Figure 9a you may observe a discontinuous change of user position and quite low positioning accuracy that corresponds to BLE-based system. There is a drift of the trajectory caused by the residual noise of the gyroscope (Figure 9b). This is typical situation for IMU-based indoor navigation systems. Finally, as was expected, the best performance is shown by HILN based on particle filter. It provides very accurate positioning with no visible track drifting in time. In all experiments held with HILN, the accuracy positioning error varied in the range 0.5 to 1 meter on an area of 15×6 meters, which is competitive to the leading commercial solutions.

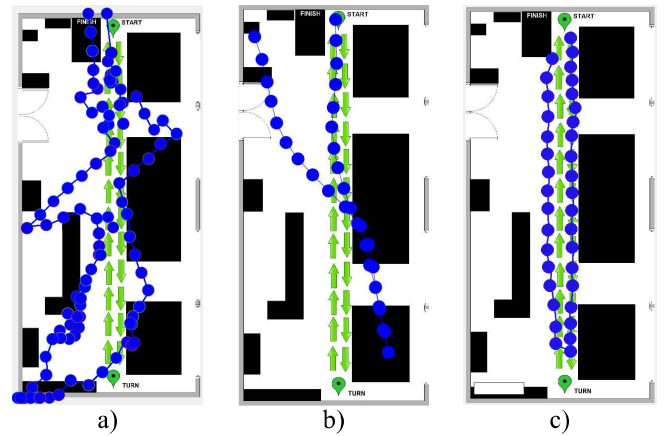


Fig. 9. Example of user position tracking performed by BLE-based system (a), IMU-based system (b) and HIL navigation system based on particle filter (c)

#### V. CONCLUSIONS

The indoor navigation is a prospective area for researching and commercializing the results of the researches as there is no unique opinion about the methods that must be used. The progress in the indoor navigation systems is provided the special techniques of signal processing, some of which were presented in current paper.

#### REFERENCES

- [1] A. Ali and N. El-Sheimy, “Low-Cost MEMS-Based Pedestrian Navigation Technique for GPS-Denied Areas,” *Journal of Sensors*, vol. 2013, Article ID 197090, 10 pages, 2013. doi:10.1155/2013/197090.

- [2] T. Zengshan, Z. Yuan, Z. Mu, and L. Yu, "Pedestrian dead reckoning for MARG navigation using a smartphone." *EURASIP J. Adv. Sign. Process.*, vol. 1, pp. 1–9, 2014.
- [3] A. Ali, and N. El-Sheimy, "Low-cost MEMS-based pedestrian navigation technique for GPS-denied areas," *Journal of Sensors*, 10 pages, 2013. 10.1155/2013/197090.
- [4] G. Trein, N. Singh, and P. Maddila, "Simple approach for indoor mapping using low-cost accelerometer and gyroscope sensors," *DOCPLAYER*, 2013.
- [5] H. Bao and W.-Ch. Wong "A Novel Map-Based Dead-Reckoning Algorithm for Indoor Localization," *Journal of Sensor and Actuator Network*, vol. 3, pp. 44–63, 2014. doi:10.3390
- [6] H. Weinberg, *Using the ADXL202 in Pedometer and Personal Navigation Applications*. Analog Devices, Inc.; Norwood, MA, USA: 2002.
- [7] Q. Tian, Z. Salcic, K.I.-K. Wang, and Y. Pan, "A Multi-Mode Dead Reckoning System for Pedestrian Tracking Using Smartphones," *IEEE Sens. J.*, vol. 16, pp. 2079–2093, 2016. doi: 10.1109/JSEN.2015.2510364.
- [8] N.-H. Ho, P. H. Truong, and G.-M. Jeong, "Step-Detection and Adaptive Step-Length Estimation for Pedestrian Dead-Reckoning at Various Walking Speeds Using a Smartphone," *Sensors*, Basel, Switzerland, vol. 16(9), pp. 1423, 2016.. <http://doi.org/10.3390/s16091423>
- [9] S.O.H. Madgwick, *An efficient orientation filter for inertial and inertial/magnetic sensor arrays*. 2010.
- [10] R. Mahony, T. Hamel, and J.-M. Pflimlin, "Complementary filter design on the special orthogonal group SO(3)," *Proceedings of the 44th IEEE Conference on Decision and Control, and the European Control Conference 2005 Seville, Spain, December 12–15, 2005*.
- [11] S. Mau, "What is the Kalman Filter and How can it be used for Data Fusion?" *Robotics Math*, pp. 16–811, December 2005.
- [12] M. Pedley, "Tilt Sensing Using a Three-Axis Accelerometer," *Freescale Semiconductor*, AN3461, 2013.
- [13] R. Zhi, *A Drift Eliminated Attitude & Position Estimation Algorithm In 3D*. Graduate College Dissertations and Theses, University of Vermont, 2016.
- [14] F. Abyarjoo, A. Barreto, J. Cofino, and F. R. Ortega, "Implementing a Sensor Fusion Algorithm for 3D Orientation Detection with Inertial/Magnetic Sensors." In: Sobh T., Elleithy K. (eds) *Innovations and Advances in Computing, Informatics, Systems Sciences, Networking and Engineering*. Lecture Notes in Electrical Engineering, vol 313. Springer, Cham. 2015, pp. 305–310.
- [15] F. Zafari, I. Papapanagiotou, M. Devetsikiotis, and T. Hacker "An iBeacon based Proximity and Indoor Localization System," *arXiv:1703.07876v2 [cs.NI]* 24 Mar 2017.
- [16] K. Vadivukkarasi, R. Kumar and Mary Joe, "A Real Time Rssi Based Novel Algorithm to Improve Indoor Localization Accuracy for Target Tracking in Wireless Sensor Networks," *ARNP Journal of Engineering and Applied Sciences*, vol. 10, no. 16, pp. 7015–7023, SEPTEMBER 2015.
- [17] T. Qinglin et al. "A Hybrid Indoor Localization and Navigation System with Map Matching for Pedestrians Using Smartphones." Ed. Kourosh Khoshelham and Sisi Zlatanova. *Sensors* (Basel, Switzerland) 15.12 (2015): 30759–30783. PMC. Web. 14 Mar. 2018.
- [18] A. Masse, S. Lefèvre, R. Binet, S. Artigues, G. Blanchet, and S.Baillarin, "Denoising Very High Resolution Optical Remote Sensing Images: Application and Optimization of Nonlocal Bayes method," *IEEE Journal of Selected Topics in Applied Earth Observations and Remote Sensing*, vol. 11:3, pp. 691–700, 2018.
- [19] T. Singhal, A. Harit, and D. N. Vishwakarma, "Kalman Filter Implementation on an Accelerometer sensor data for three state estimation of a dynamic system," *International Journal of Research in Engineering and Technology (IJRET)*, vol. 1, no. 6, 2012. ISSN 2277 – 4378
- [20] P. Del Moral, "Non Linear Filtering: Interacting Particle Solution". *Markov Processes and Related Fields*. 2 (4) pp. 555–580, 1996.
- [21] B.I. Ahmad, J. Murphy, P.M. Langdon, and S. J. Godsill, "Filtering perturbed in-vehicle pointing gesture trajectories: Improving the reliability of intent inference", *Machine Learning for Signal Processing (MLSP) 2014 IEEE International Workshop on*, pp. 1–6, 2014.
- [22] D. Gusenbauer, C. Isert, and J. Krosche, "Self-contained indoor positioning on off-the-shelf mobile devices," *International Conference on Indoor Positioning and Indoor Navigation (IPIN)*, pp. 1–9, 2010.